Green Chemistry

PAPER

View Article Online
View Journal | View Issue

Check for updates

Cite this: *Green Chem.*, 2024, **26**, 5890

Mechanochemical aerobic oxidative Heck coupling by polymer-assisted grinding: cyclodextrin additive facilitating regioselectivity control†

Keyu Xiang, [a] Haowen Shou,[a,b] Chenhui Hu,[a] Weike Su [a] and Jingbo Yu *[a]

The oxidative Heck reaction is a well-known organic transformation. However, previous reactions have been limited by the need for sophisticated directing or auxiliary groups, reliance on bulk solvents, lack of catalyst recycling, and the formation of a mixture of isomeric products, thereby hindering its broader application. Herein, we present a novel approach utilizing the polymer-assisted grinding (POLAG) technique to facilitate the regioselective oxidative Heck coupling of aryl boronic acids with electronically unbiased olefins under solvent-free conditions. This catalytic reaction is facilitated by a ligand-free Pd $(TFA)_2$ catalyst in conjunction with cyclodextrin (CD) serving as a POLAG additive and molecular oxygen as the green oxidant. Mechanistic studies have indicated that cyclodextrin not only stabilizes the palladium catalyst but also influences the reaction selectivity by imposing steric hindrance on the substrates. Recovery experiments and electron microscopy images demonstrate an effective recovery capability of Pd/CD, with the catalyst morphology largely preserved after five cycles. XPS experiments confirm the formation of a new palladium catalytic species during the ball-milling process. Remarkably, this reaction takes place at ambient temperature, obviating the need for additional stoichiometric amounts of hazardous oxidants and toxic solvents, aligning with environmentally friendly practices upon green metrics evaluation.

Received 28th February 2024,
Accepted 3rd April 2024

DOI: 10.1039/d4gc01006j

rsc.li/greenchem

Published on 09 2024. Downloaded on 26-11-2025 15:26:21.

Introduction

The emergence of mechanochemical synthesis as an efficient and sustainable technology has been witnessed in recent decades.[1,2] This technology has been recognized by the International Union of Pure and Applied Chemistry (IUPAC) in 2019 as one of the top ten emerging technologies in the field of chemistry for its potential to advance society and improve our quality of life.[3] In comparison with traditional solution-based methods, the mechanochemical protocol provides numerous advantages such as minimal solvent usage, milder conditions, shorter reaction time and the capability to alter chemical reactivity and selectivity, thereby leading to a reduced environmental footprint and favourable results in green metric assessment.[4,5]

Some mechanochemical reactions exhibit unique chemical behaviours and different reaction pathways when a small amount of additive is introduced.[1h,6] These reactions can be classified into two distinct groups. First, a specialized approach to mechanochemical reactions that involves the use of catalytic liquid additives, known as liquid-assisted grinding (LAG),[7,8] which was introduced nearly two decades ago and has been shown to significantly enhance reaction rates and reactivity (Fig. 1a). For instance, Browne and co-workers[9] reported an elegant finding when using LAG to selectively favor mono-fluorination over di-fluorination in the presence of a catalytic amount of acetonitrile. Our recent work[10] on LAG reactions demonstrated that trace amounts of *tert*-butanol could accelerate the asymmetric C_{sp^3}–H/C_{sp^3}–H coupling of glycine esters and β-indanone esters, wherein *tert*-butanol not only provides a sub-stoichiometric solvent environment, but also contributes to the formation of active transition species, thereby boosting catalytic activity and enantiocontrol.

The other type of mechanochemical technique, which utilizes polymer additives to improve chemical transformations

[a]*Laboratory of Pharmaceutical Engineering of Zhejiang Province, Key Laboratory for Green Pharmaceutical Technologies and Related Equipment of Ministry of Education, Collaborative Innovation Center of Yangtze River Delta Region Green Pharmaceuticals, Zhejiang University of Technology, Hangzhou, 310014, P. R. China. E-mail: yjb@zjut.edu.cn*

[b]*State Key Laboratory of Drug Research, Shanghai Institute of Materia Medica, Chinese Academy of Sciences, Shanghai, 201203, P.R. China*

†Electronic supplementary information (ESI) available: Experimental procedures, optimization data, mechanism study, ICP-MS and XPS analyses, green metrics calculation, characterization data and NMR spectra. See DOI: https://doi.org/10.1039/d4gc01006j

This journal is © The Royal Society of Chemistry 2024

Published on 09 2024. Downloaded on 26-11-2025 15:26:21.

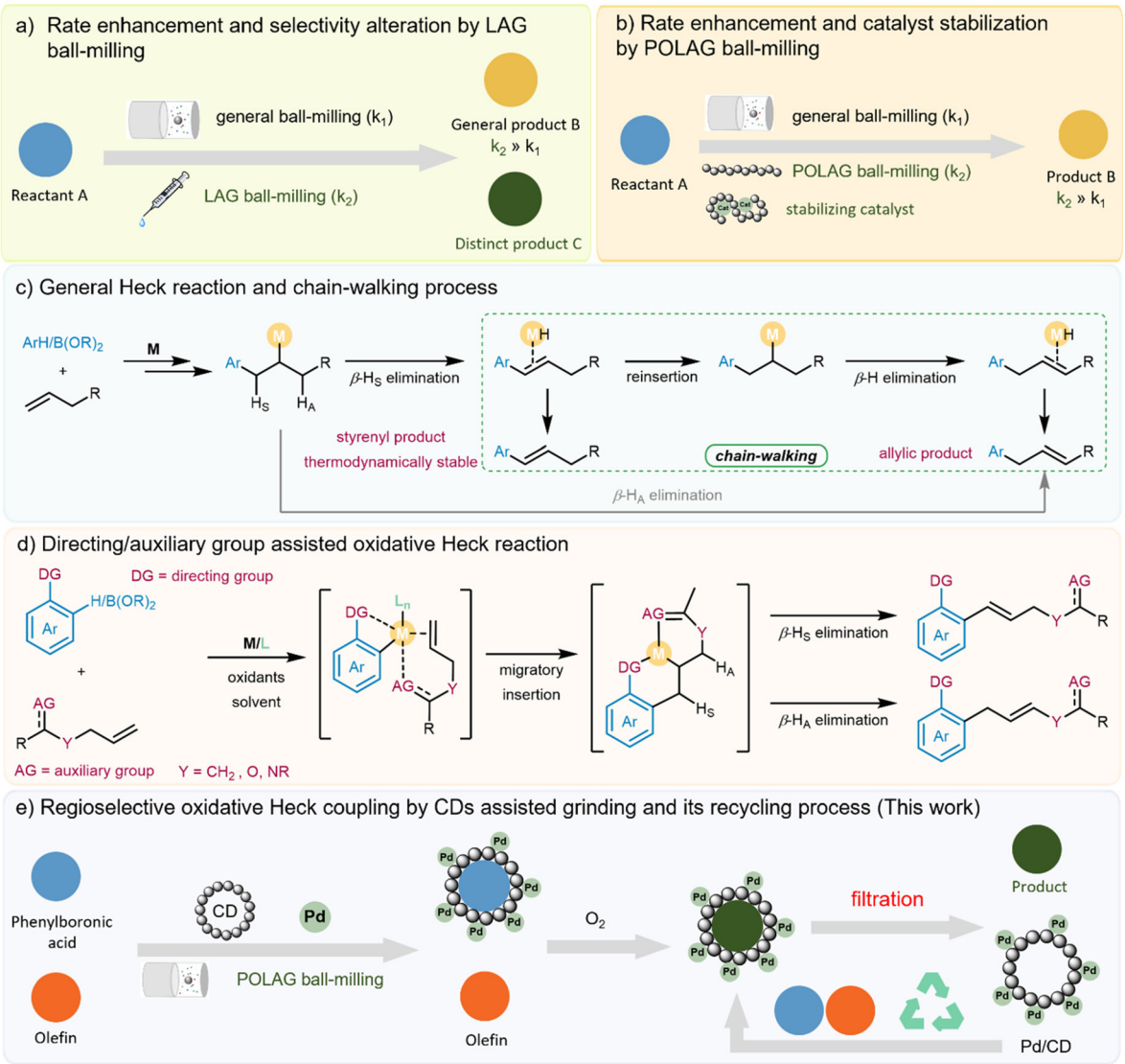

Fig. 1 (a) Rate enhancement and selectivity alteration by LAG ball-milling. (b) Rate enhancement and catalyst stabilization by POLAG ball-milling. (c) General Heck reaction and chain-walking process. (d) Directing/auxiliary group assisted oxidative Heck reaction. (e) Regioselective oxidative Heck coupling by CD assisted grinding and its recycling process (this work).

by stabilizing catalysts or altering intermolecular interactions, is referred to as polymer-assisted grinding (POLAG)[11] (Fig. 1b). A representative example was showcased by Lamaty and co-workers[12] using polyethylene glycol (PEG) additives to accelerate the palladium-catalyzed Mizoroki–Heck cross-coupling reaction for the first time, leading to a significant improvement in reaction efficiency. More recently, the Ito group[2i] reported that the use of the PEGylated phosphine ligand in POLAG could effectively suppress the deactivation of palladium in a Suzuki–Miyaura coupling reaction. Despite advances, these methods are still facing sustainability challenges, primarily due to the lack of emphasis on the recycling of additives/catalysts, leading to unsatisfactory results in green metric assessments. In these scenarios, some polymer-assisted grindings using natural source additives, such as saccharides, have attracted our attention.[13] Considering that saccharides can act as reducing agents under ball-milling conditions,[13a] we envision that such POLAG could also be used to facilitate catalytic redox processes to enable selectivity control through topology matching between the oligosaccharide additives and the substrates, or by forming a specific metal–additive complex.

On the other hand, the oxidative Heck-type reaction is one of the most attractive transformations that converts vinylic C–H bonds into C–C bonds, finding wide applications in synthetic chemistry.[14] However, a serious limitation is that the use of inactive alkenes often leads to an inseparable mixture of styrene/allylic isomers. This issue primarily results from a chain-walking process,[15] wherein reinsertion of the metal-hydride species is followed by β-hydride elimination. Moreover, imperfect selectivity also arises from the inability of

Published on 09 2024. Downloaded on 26-11-2025 15:26:21.

metal-hydride species to distinguish between H_S and H_A during β-hydride elimination[14c,16] (Fig. 1c). Over the past few years, a wealth of methods for the regulation of the oxidative Heck-type reactions involving electronically unbiased olefins have been developed by the groups of White,[17] Liu,[18] Xu,[19] Yu,[20] Maiti,[21] Jeganmohan,[22] Sigman[23] and others.[24] The selectivity aspect of these transformations can be affected by the use of a specially designed ligand, which has proved to be an attractive tool for achieving catalyst recycling in some cases.[24c,d] Nevertheless, there often remains a necessity for stoichiometric hazardous oxidants, bulk solvent, and preinstalled auxiliary/directing groups (Fig. 1d). Such requirements greatly limit the utility of the oxidative Heck reaction. The development of an operationally simple protocol for oxidative Heck coupling without the need for solvent, ligands, toxic oxidant and auxiliary/directing groups would therefore be highly beneficial.

We herein report a practically useful mechanochemical strategy for solvent-free oxidative coupling of phenylboronic acid with electronically unbiased olefins using polysaccharides as POLAG additives (POLAGs) under an oxygen atmosphere (Fig. 1e). We found that commercial cyclodextrins (CDs) were capable of regulating the regioselectivity of the oxidative Heck reaction *via* interactions between the substrates and the CD cavity, as well as through the formation of a new metal/CD complex *in situ*. The inclusion of CD not only led to high dispersion of the substrate within the solid mixture but also facilitated the stabilization of the metal catalysts. To the best of our knowledge, there have been no reports thus far regarding the selective oxidative Heck reaction with unbiased olefins under solvent-free mechanochemical conditions. Furthermore, the use of oxygen as a green oxidant, CD as a renewable natural additive for POLAG, which can be recycled and reused alongside the metal catalyst, aligns this protocol with the principles of green chemistry.

Table 1 Optimization of the reaction conditions[a]

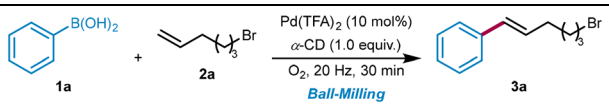

Entry	Variation	Yield[f]
1	None	30
2	$Pd(OAc)_2$ instead of $Pd(TFA)_2$	22
3	$Pd[O_2C(CH_3)_3]_2$ instead of $Pd(TFA)_2$	Trace
Variation of additive		
4	β-CD instead of α-CD	20
5	γ-CD instead of α-CD	17
6	Methyl α-D-glucopyranoside instead of α-CD	Trace
7	α-Lactose instead of α-CD	Trace
8	Soluble starch instead of α-CD	21%
9	2.0 equiv. α-CD	Trace
10	0.8 equiv. α-CD	51
11	0.6 equiv. α-CD	57
12	**0.4 equiv. α-CD**	**63**
13	0.2 equiv. α-CD	50
14	Without CD	10
Reaction in the presence of 0.4 equiv. α-CD		
15	5 mol% $Pd(TFA)_2$	22
16	7 mol% $Pd(TFA)_2$	46
17[b]	O_2 flow rate (4/6/8 mL min^{-1})	51/63/63
18	Milling ball sizes (∅ = 1.0/1.4 cm)	59 (57[c])/63
19[d]	10 mol% $Pd(TFA)_2$	9%
20[e]	10 mol% $Pd(TFA)_2$	Trace

[a] Reaction conditions: **1a** (0.5 mmol), **2a** (0.5 mmol), $Pd(TFA)_2$ (10 mol%) and an additive were placed in a 25 mL stainless-steel jar with two stainless-steel balls (∅ = 1.2 cm), milling at 20 Hz for 30 min under an oxygen atmosphere. [b] A gas flowmeter was utilized to precisely monitor and regulate the oxygen flow rate. [c] 50 mL stainless-steel jar was used. [d] Comparative experiment: **1a** (0.5 mmol), **2a** (0.5 mmol), $Pd(TFA)_2$ (10 mol%), α-CD (0.4 equiv.) and DMF (5 mL) were added in a round-bottomed flask, stirring at 50 °C for 24 h under an oxygen atmosphere. [e] Comparative experiment: **1a** (0.5 mmol), **2a** (0.5 mmol), $Pd(TFA)_2$ (10 mol%) and α-CD (0.4 equiv.) were placed in a stainless-steel jar without agitation for 4 h under an oxygen atmosphere, then aged in an flask for 7 days under an oxygen atmosphere. [f] Isolated yields.

Results and discussion

The initial studies of the oxidative Heck reaction involved the utilization of phenylboronic acid (**1a**) and 6-bromo-1-hexene (**2a**) as coupling substrates in the presence of $Pd(TFA)_2$ (10 mol%), and α-CD (1.0 equiv.) under flowing oxygen. The reaction was conducted in a custom-made ventilated stainless-steel jar (see the ESI† for details) under optimized mechanical parameters (20 Hz, 30 min, see Fig. S1†). After screening several metal catalysts, we found that $Pd(TFA)_2$ gives the desired product in 30% yield (Table 1, entries 1–3). Further additive screening indicated that only CDs and soluble starch led to product formation, whereas trace amounts of the product were observed when methyl α-D-glucopyranoside and α-lactose were used as POLAGs (Table 1, entries 4–8). We also surveyed the molar amount of α-CD (Table 1, entries 9–14), finding that while excess α-CD inhibited the formation of the product, lowering its equivalence to 0.2 and 0.1 also led to significant decreases of yield. Moreover, reducing the amount of $Pd(TFA)_2$ in the presence of α-CD lowered the yield of **3a** (Table 1, entries 15 and 16). It is worth noting that both the oxygen flow rate and the size of milling balls significantly impact the reaction outcomes. In Table 1, entry 17 demonstrates that augmenting the oxygen flow rate from 4 to 8 mL min^{-1} correspondingly increases the reaction yield, achieving peak conversion under an oxygen flow of 6 mL min^{-1} (for more details, see ESI section 3.2†). Conversely, reducing the ball size to ∅ 1.0 cm notably hampers the reaction efficiency, especially in a larger 50 mL milling jar, likely due to a decrease in the mechanical force that results in inferior dispersion of reagents and increased aggregation (for more details, see ESI section 3.3†). However, using even larger balls with ∅ 1.4 cm did not lead to any additional enhancement (Table 1, entry 18). Our control experiments are depicted in entries 19 and 20, which were a subset of reactions that were conducted in a round-bottomed flask. It is noteworthy that stirring the reaction mixture in a DMF solution resulted in a heterogeneous

 This journal is © The Royal Society of Chemistry 2024

Published on 09 2024. Downloaded on 26-11-2025 15:26:21.

state and led to poor conversion to the alkenylation product **3a**. To understand the role of agitation during the ball-milling process, gaseous oxygen was flushed over the mixture of **1a**, **2a**, α-CD and $Pd(TFA)_2$ for **4h** without any agitation, followed by storing the mixture under an O_2 atmosphere at ambient pressure for 7 days. No transformation was observed after the "aging"[25] process (Table 1, entry 20), confirming that the milling process is necessary for the conversion.

With the optimal reaction conditions in hand, we set out to explore the scope of functionalized aliphatic olefins **2** in the oxidative Heck reaction, using **1a** as a model substrate (Scheme 1). The mild reaction conditions allowed for the tolerance of a wide range of functional groups, including alkyl bromine (**3a**), alcohol (**3b**), ether (**3c**), acid (**3d**), ester (**3e**), amide (**3f**) and aryl groups (**3h–3j**). All reactions delivered the styrenyl products with exclusive *E*-stereoselectivity. Owing to the lack of chelation/directing effects, performing a ligand-free oxidative Heck reaction with electronically unbiased olefins is generally challenging. Such reactions have been rarely reported in the literature, typically achieving unsatisfactory yield and selectivity.[26] Unfortunately, this synthesis was found to be barely suitable for substituted arylboronic acids. While some arylboronic acids with different substituents exhibited excellent selectivity and satisfactory yields when coupled with methyl 3,3-dimethylpent-4-enoate (**3k–3p**), undesired isomers (allylic and branch) were observed when using other olefins (for details see ESI Scheme S1†).

We further elaborated the scope of this reaction with several aliphatic olefins derived from natural products and active pharmaceutical ingredients. Specifically, the substituted

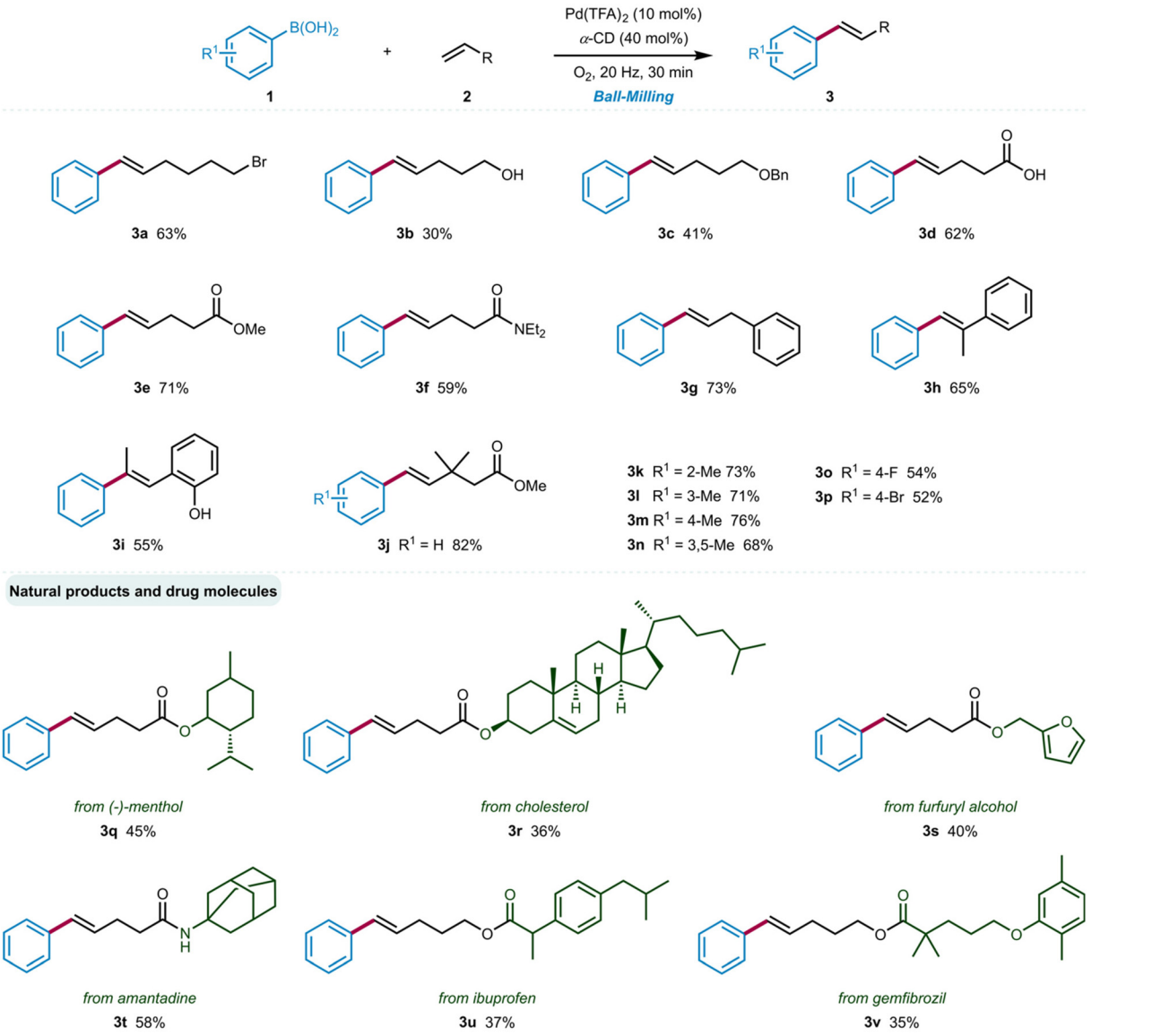

Scheme 1 Substrate scope for the functionalized aliphatic olefins. Reaction conditions: **1** (0.5 mmol), **2** (0.5 mmol), $Pd(TFA)_2$ (10 mol%), and α-CD (40 mol%) were placed in a stainless-steel vessel with two stainless-steel balls (⌀ = 1.2 cm) milling at 20 Hz for 30 min under an oxygen atmosphere. Isolated yields.

Published on 09 2024. Downloaded on 26-11-2025 15:26:21.

olefins obtained from menthol (**3q**), cholesterol (**3r**), furfuryl alcohol (**3s**), and the embedded olefins in amantadine (**3t**), ibuprofen (**3u**), and gemfibrozil (**3v**) produced the expected products in 35–58% yields, highlighting the excellent functional group compatibility of this strategy.

A wide range of unfunctionalized aliphatic olefins were then examined (Scheme 2), including long linear olefins (**5a–5c**), branched olefins (**5d–5h**, **5j**), camphene (**5i**), exocyclic olefin (**5k**) and cyclic olefins (**5l–5n**). They all demonstrated excellent reactivity and yielded the *E*-styrenyl products with high selectivity. The longer-chain olefins gave the target product in a slightly higher yield than the shorter ones (**5c** > **5b** > **5a**). The use of phenylboronic acid with different substituents also yielded the desired products **5d–5h** in good yield. Initially, relatively low yields were obtained, possibly due to the emission of neohexene (bp. 41 °C) during the milling process under flowing oxygen. As anticipated, increasing the amount of neohexene to 2 equiv. led to the desired products in high yields (up to 85%), and the products could be easily isolated by filtration and distillation (for details, see ESI section 3.6†). Interestingly, under the standard conditions, cyclopentene (**4l**) hardly participated in the reaction, yielding no product. However, when employing β-CD instead of α-CD, an allylic-type product **5l** was obtained in 70% yield. Similarly, the reactions with cyclohexene and cyclooctene produced the allylic products **5m** and **5n** with yields of 68% and 74%, respectively.

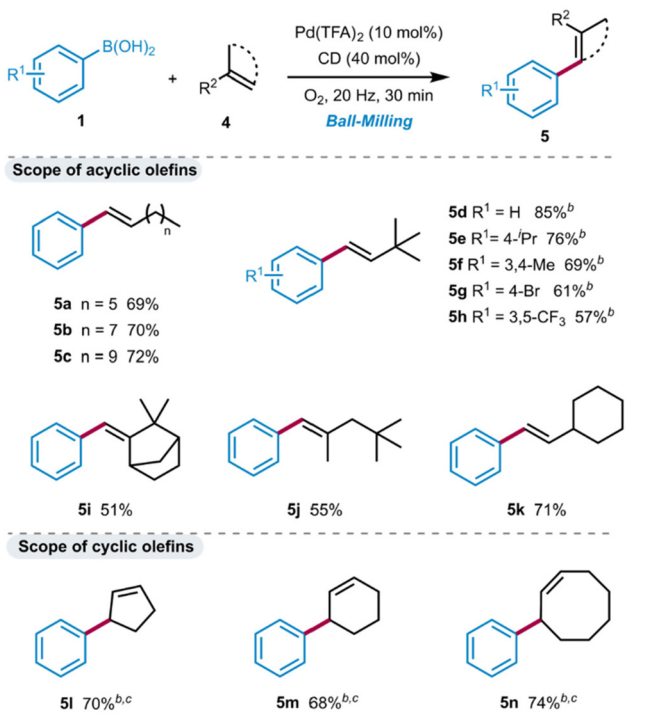

Scheme 2 Substrate scope for the unfunctionalized aliphatic olefins.[a] [a] Reaction conditions: **1** (0.5 mmol), **4** (0.5 mmol), $Pd(TFA)_2$ and α-CD (40 mol%) were placed in a stainless-steel vessel with two stainless-steel balls (⌀ = 1.2 cm) milling at 20 Hz for 30 min under an oxygen atmosphere. Isolated yields. [b] Two equiv. of olefins were added. [c] β-CD was used instead of α-CD.

In the previous report, it was suggested that the size of the CD cavity significantly influences the reaction selectivity.[13d,e] To validate this hypothesis, we expanded the study to include several substrates with varying sizes of CDs. The results of the reaction between 6-bromine-1-hexene (**2a**) and phenylboronic acid (**1a**) are shown in Fig. S6.† When α-CD was used as the POLAG additive, only the styrenyl product **3a** was formed, whereas when β-CD was used it led to a mixture of styrenyl and allylic products. No products were detected when γ-CD was utilized. In the absence of POLAGs, the reaction afforded a mixture of styrenyl, allylic, branched, and homocoupled products, highlighting the significant role of CD in regulating the selectivity for this oxidative Heck reaction. Additionally, the reactions between phenylboronic acid (**1a**) and camphene (**4i**), cyclopentane (**4l**) or cyclooctene (**4n**) were also carried out with or without the addition of α-CD/β-CD/γ-CD. The reactivity and selectivity of the POLAG reaction were found to be highly dependent on the matching of the cavity size of the CD and the substrate (for more details, see ESI sections 3.3 and 4†).

Next, the recyclability of the Pd/α-CD catalyst was examined in the reaction of phenylboronic acid (**1a**) and olefins **2j**/**4c**/**4d**/**4i** (see ESI Fig. S11†). The results showed that Pd/α-CD can be reused in five runs without significant loss of efficiency. After each run, Pd/α-CD was recovered by washing with cyclohexane, dried under vacuum, and directly used for the next reaction. However, a slight loss of yield was observed after five cycles, potentially due to the loss of Pd content during the recycling process (for ICP-MS results, see ESI Table S3†).

Moreover, in order to rule out the potential catalytic effects stemming from leached metals such as Fe, Co, and Ni present in stainless-steel materials during the mechanochemically activated reaction, control experiments were carried out using alternative zirconium oxide/Teflon jars and balls. These tests revealed that there was virtually no discernible difference in the reaction outcome between jars and balls made of stainless-steel *versus* those made of zirconium (for details, see ESI section 3.11†). It is noteworthy that the observed decrease in yield with the Teflon jar could be attributed to the lower mechanical force exerted due to its lighter weight material.

To gain mechanistic insight into the observed catalytic effect upon the addition of CD, we used scanning electron microscopy (SEM) to confirm the changes in the microstructures of the Pd/CD mixture. In Fig. 2a, a high dispersion of palladium with CD is evident after the first run of the Pd/CD mixture, whereas Fig. 2b depicts a decrease in the dispersion density of Pd after 5 runs, indicating the possibility of the loss of Pd content during the recycling process, which is consistent with the ICP-MS results. However, the Pd catalyst remained attached to α-CD even after 5 runs, which was tentatively confirmed by energy-dispersive spectroscopy (EDS) mapping experiments, as shown in Fig. 2c–f. These EDS mapping results showed a uniform distribution of Pd, C and O in the Pd/CD mixture, suggesting that $Pd(TFA)_2$ and α-CD may form relatively stable Pd/CD dispersions/complexes after mechanochemical ball-milling, with α-CD potentially serving as a dispersant for the Pd catalyst.

 This journal is © The Royal Society of Chemistry 2024

Published on 09 2024. Downloaded on 26-11-2025 15:26:21.

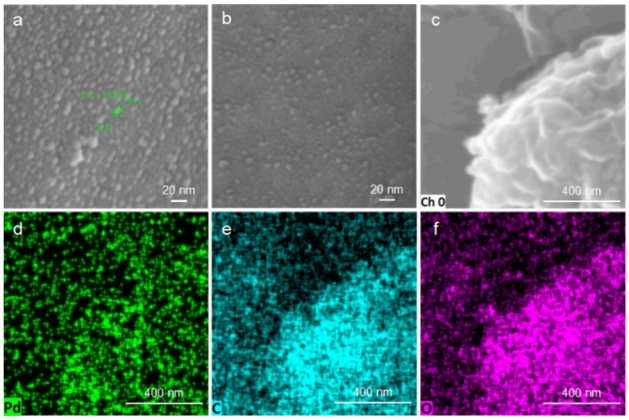

Fig. 2 Scanning electron microscopy images of the Pd/α-CD (a) after the first run and (b) after the fifth run. (c–f) EDS-SEM images of the Pd/α-CD after the fifth run.

Transmission electron microscopy (TEM) was further utilized to validate the *in situ* generation of Pd/CD dispersions/complexes during the ball-milling process (Fig. 3). The observed images clearly show the formation of evenly distributed Pd nanoparticles on CD in the reaction mixture (Fig. 3a). The morphology of Pd/CD remained unchanged over 5 consecutive catalytic runs, with only a slight aggregation of the Pd particles observed (Fig. 3c), and no significant alteration in particle size (approximate size: 2–4 nm).

On the other hand, the image obtained for the palladium species derived from the reaction mixture in the presence of α-D-glucopyranoside, α-lactose monohydrate and soluble starch (Fig. 4) indicates significant aggregation of the Pd species into dense particles (Fig. 4). These findings suggest that α-CD might act as a dispersant for the Pd-based catalyst to inhibit excessive aggregation of the nanoparticles.

For further investigation of the interaction between Pd catalyst and α-CD, X-ray photoelectron spectroscopy (XPS) was carried out for the commercial $Pd(TFA)_2$ (Fig. 5a), $Pd(TFA)_2$/

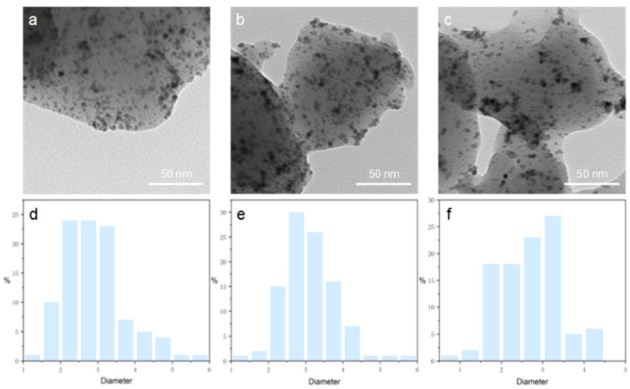

Fig. 3 Transmission electron micrographs of the Pd/α-CD and size distributions. (a) After the first run; (b) after the third run; (c) after the fifth run; (d) size distributions for a; (e) size distributions for b; (f) size distributions for c.

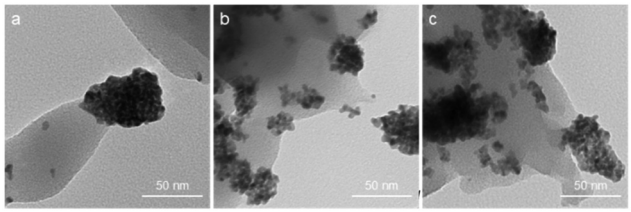

Fig. 4 Transmission electron micrographs of the Pd catalyst with saccharide additives after the first run. (a) Pd/methyl α-D-glucopyranoside, (b) Pd/α-lactose monohydrate, (c) Pd/soluble starch.

α-CD (*Sample A*, Fig. 5b), reaction mixture with CD (*Sample B*, Fig. 5c), and reaction mixture without CD (*Sample C*, Fig. 5d). As determined by XPS, the binding energy of Pd 3d 5/2 in *Sample A* (for Pd II, 336.64 eV) was lower than that in $Pd(TFA)_2$ (for Pd II, 338.17 eV), which is attributed to $Pd^{II}O$ species and comparable to the literature binding energy value in the NIST X-ray photoelectron spectroscopy database.[27] The presence of the $Pd^{II}O$ peak indicates that the formation of the new catalyst takes place after ball-milling with α-CD (*Sample A*, Fig. 5b). Besides, $Pd^{II}O$ species were also observed in the reaction mixture with CD (*Sample B*), with appropriate amounts of metallic Pd^0 formed (Fig. 5c). For the reaction mixture without CD (*Sample C*), only $Pd(TFA)_2$ and Pd(0) species were confirmed by XPS, and no signal characteristic of $Pd^{II}O$ was detected (Fig. 5d).

From the above observations, we can conclude that a new Pd–O bond was formed between $Pd(TFA)_2$ and CD induced by mechanical force, leading to the formation of stable Pd/CD complexes. These complexes can stabilize the Pd(0) originating from the reductive elimination process and facilitate its re-oxidation to Pd(II), thereby improving the catalytic efficiency of the reaction. Conversely, in the absence of CD, the catalytic efficiency of $Pd(TFA)_2$ was suppressed, and the re-oxidation of the deactivated Pd(0) was challenging due to aggregation, which significantly inhibited the catalytic cycle (see also Table 1, entry 14).

Finally, a direct comparison of this work with previous literature studies[28] is shown in Fig. 6. Our POLAG reaction demonstrated time economy and avoids the use of bulky solvents and purpose-made catalysts. The formation of (*E*)-5-phenylpent-4-enoic acid (**3d**), (*E*)-prop-1-ene-1,3-diyldibenzene (**3g**), (*E*)-prop-1-ene-1,2-diyldibenzene (**3h**), and (*E*)-(3,3-dimethylbut-1-en-1-yl)benzene (**5d**) highlights the avoidance of severe conditions to facilitate the transformations (80–140 °C *vs.* rt). In the case of solvent-free oxidative Heck coupling, our previous conditions utilized DDQ as the oxidant.[28d] Mechanochemical olefinations with methyl 3,3-dimethylpent-4-enoate, 3,3-dimethylbut-1-ene and neohexene under an oxygen atmosphere are all illustrative of the greenness of this methodology as compared to our previous approach.

Moreover, various green metrics, including effective mass yield (EMY), atom economy (AE), atom efficiency (AEF), reaction mass efficiency (RME), optimum efficiency (OE), process mass intensity (PMI), mass intensity (MI), solvent intensity

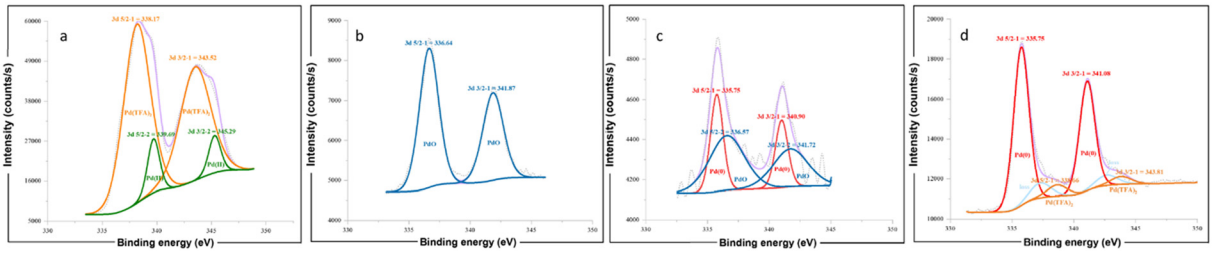

Fig. 5 X-ray photoelectron spectroscopy of the mixtures after the reaction. (a) Commercial $Pd(TFA)_2$; (b) the mixture of $Pd(TFA)_2$ and α-CD after 30 min ball-milling at 20 Hz; (c) the mixture of $Pd(TFA)_2$, olefin, phenylboronic acid and α-CD after 30 min ball-milling at 20 Hz, followed by rinsing with cyclohexane and drying; (d) the mixture of $Pd(TFA)_2$, olefin and phenylboronic acid after 30 min ball-milling at 20 Hz, followed by rinsing with cyclohexane and drying.

Published on 09 2024. Downloaded on 26-11-2025 15:26:21.

This work	Substrates	Literature conditions
$Pd(TFA)_2$ (0.1 eq), O_2 α-CD (0.4 eq), rt, 30 min 62%	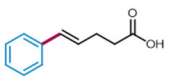 3d	1) $Pd(OAc)_2$ (0.02 eq), Et_3N (2 eq) PPh_3 (0.96 eq), 80 °C, 3 h 2) HCl (aq) 54%[28a]
$Pd(TFA)_2$ (0.1 eq), O_2 α-CD (0.4 eq), rt, 30 min 73%	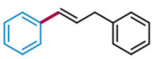 3g	1) $Pd(OAc)_2$ (0.1 eq), Et_3N (50 mL) P(*o*-tol)$_3$ (0.4 eq), 80 °C, 10 h 2) $NaHCO_3$ (aq), EA 44%[28b]
$Pd(TFA)_2$ (0.1 eq), O_2 α-CD (0.4 eq), rt, 30 min 65%	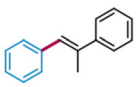 3h	[Pd(II)(N,O)$_2$] complex (0.05 eq) Na_2CO_3 (1 eq), DMF (1 mL) 140 °C, 24 h 53%[28c]
$Pd(TFA)_2$ (0.1 eq), O_2 α-CD (0.4 eq), rt, 30 min 82%	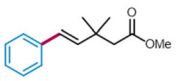 3j	$Pd(OAc)_2$ (0.1 eq), TCA (1 eq) DDQ (0.2 eq), SiO_2 (0.4 g), rt, 30 min 44%[28d] Pd@POP (0.001 eq), DMA (4 mL) $Cu(OTf)_2$ (0.2 eq), O_2, 40 °C, 48 h 81%[24d]
$Pd(TFA)_2$ (0.1 eq), O_2 α-CD (0.4 eq), rt, 60 min 69%	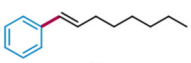 5a	Pd@POP (0.001 eq), DMA (4 mL) $Cu(OTf)_2$ (0.2 eq), O_2, 40 °C, 48 h 67%[24d]
$Pd(TFA)_2$ (0.1 eq), O_2 α-CD (0.4 eq), rt, 60 min 85%	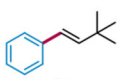 5d	$Pd(OAc)_2$ (0.1 eq), TCA (1 eq) DDQ (0.2 eq), SiO_2 (0.4 g), rt, 30 min 42%[28d] $InCl_3$ (0.05 eq) AcONa (1 eq) DMF (2 mL), 140 °C, 24 h 80%[28e]
$Pd(TFA)_2$ (0.1 eq), O_2 α-CD (0.4 eq), rt, 60 min 55%	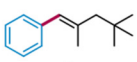 5j	$Pd(OAc)_2$ (0.1 eq), TCA (1 eq) DDQ (0.2 eq), SiO_2 (0.4 g), rt, 30 min 43%[28d]
$Pd(TFA)_2$ (0.1 eq), O_2 α-CD (0.4 eq), rt, 60 min 71%	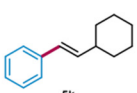 5k	COF-BTDH (0.06 eq), DMA (4 mL) $Pd(OAc)_2$ (0.06 eq), $Cu(OTf)_2$ (0.2 eq) O_2, 40 °C, 48 h 74%[24c]

Fig. 6 Direct comparison with literature processes.

This journal is © The Royal Society of Chemistry 2024

Published on 09 2024. Downloaded on 26-11-2025 15:26:21.

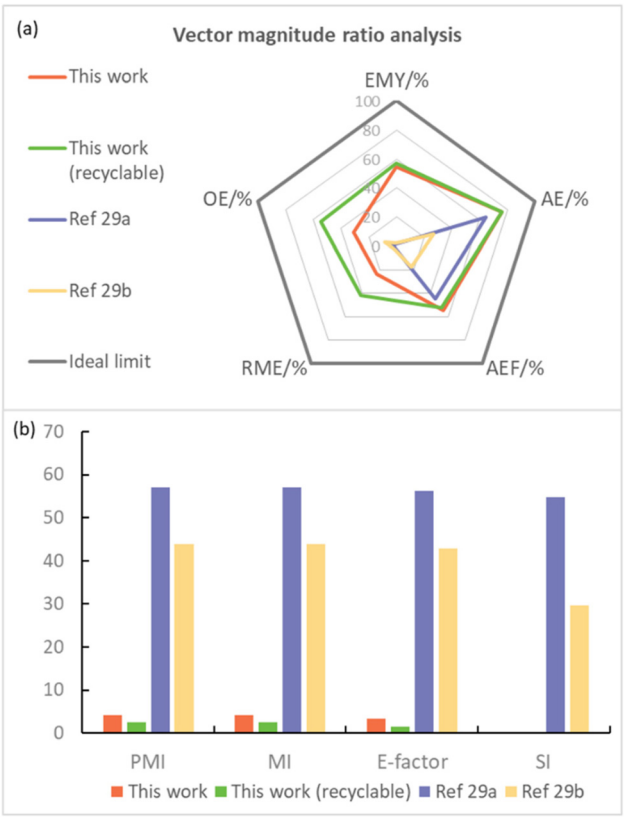

Fig. 7 Summary of green chemistry metrics. The parameters in (a): the higher the better; in (b): the lower the better.

(SI), and *E*-factor parameters, were employed to simultaneously evaluate the efficiency and environmental impact of the process in the synthesis of (*E*)-dodec-1-en-1-ylbenzene (**5c**) compared with a reported solution-based method,[29] as per the literature.[4a,30] As seen in Fig. 7a, a value of 1 for each pentagon radius is considered as the ideal condition for a sustainable process, and the closer the value of the different metrics to unity, the greener the process. In contrast, lower PMI, MI, *E*-factor, and SI scores signify a more environmentally friendly process (Fig. 7b).

It is noteworthy that the atom efficiency (AE) value is the highest for this work, probably due to the negligible contribution of lower molecular weight of the leaving group. Besides, the mechanochemical POLAG approach exhibits significantly superior parameters in terms of EMY, PMI, MI, SI and *E*-factor compared to those of previous solution-based methods. These findings underscore the importance of advancing solvent-free reactions and incorporating material recovery.

Conclusions

In this study, a mild and highly regioselective oxidative Heck cross-coupling of aryl boronic acids and electronically unbiased olefins was developed using the polymer-assisted grinding (POLAG) methodology. The method integrates eco-friendly components such as employing oxygen as an oxidant and naturally sourced cyclodextrin (CD) as a recyclable POLAG additive, establishing a sustainable and green synthesis pathway. This approach exhibits compatibility with a range of olefins that were previously ineffective in direct oxidative Heck coupling, while delivering products with excellent regioselectivity. Mechanistic study showed that cyclodextrin was efficient for the dispersion of Pd catalyst and also prevented the formation of undesired isomers. Analyses by transmission electron microscopy, scanning electron microscopy and X-ray photoelectron spectroscopy suggest the formation of a new form of $Pd^{II}O$ catalyst during the ball-milling process, which prevented catalyst deactivation caused by palladium species aggregation, despite a slight loss of palladium observed after five runs. Furthermore, the regioselectivity of the Pd/CD-catalyzed oxidative Heck coupling strongly relies on the CD/substrate interaction, suggesting topology matching between the CD and the substrate. Notably, a quantitative assessment of green chemistry metrics further demonstrates the environmental friendliness of this methodology compared to that of traditional solution-based approaches.

This study presents a sustainable approach for regioselective oxidative Heck reactions, demonstrating significant potential for the efficient and selective synthesis of organic products by a polymer-assisted grinding method.

Author contributions

JB suggested the idea. KY, HW and CH performed the experiments and the greenness evaluation. HW carried out the electron microscopy experiments and processed the data. WK and JB supervised the project. Writing – review and editing were conducted by KY and JB. All authors have read and approved the final manuscript.

Conflicts of interest

There are no conflicts to declare.

Acknowledgements

We gratefully acknowledge the Natural Science Foundation of Zhejiang Province (LY23B060005), the National Key R&D Program of China (2021YFC2101000) and the National Natural Science Foundation of China (21978270) for financial support.

References

1 For selected reviews discussing mechanochemical studies see: (*a*) V. Martinez, T. Stolar, B. Karadeniz, I. Brekalo and K. Užarević, *Nat. Rev. Chem.*, 2023, **7**, 51–65; (*b*) J. Reynes, V. Isoni and F. García, *Angew. Chem., Int. Ed.*, 2023, **62**, e2023008; (*c*) A. Jones, J. Leitch, S. Raby-Buck and

Published on 09 2024. Downloaded on 26-11-2025 15:26:21.

D. Browne, *Nat. Synth.*, 2022, **1**, 763–775; (*d*) I. Egorov, A. Mukherjee, S. Santra, D. Kopchuk, I. Kovalev, Y. Liu, G. Zyryanov, A. Majee, O. Chupakhin and B. Ranu, *Adv. Synth. Catal.*, 2022, **364**, 2462–2478; (*e*) M. Williams, L. Morrill and D. Browne, *ChemSusChem*, 2022, **15**, e2021021; (*f*) E. Colacino, V. Isoni, D. Crawford and F. García, *Trends Chem.*, 2021, **3**, 335–339; (*g*) P. Ying, J. Yu and W. Su, *Adv. Synth. Catal.*, 2021, **363**, 1246–1271; (*h*) T. Friščić, C. Mottillo and H. Titi, *Angew. Chem., Int. Ed.*, 2020, **59**, 1018–1029; (*i*) W. Pickhardt, S. Grätz and L. Borchardt, *Chem. – Eur. J.*, 2020, **26**, 12903–12911; (*j*) A. Porcheddu, E. Colacino, L. Luca and F. Delogu, *ACS Catal.*, 2020, **10**, 8344–8394; (*k*) M. Perez-Venegas and E. Juaristi, *ACS Sustainable Chem. Eng.*, 2020, **8**, 8881–8893; (*l*) N. Egorov, S. Santra, D. Kopchuk, I. Kovalev, G. Zyryanov, A. Majee, B. Ranu, V. Rusinov and O. Chupakhin, *Green Chem.*, 2020, **22**, 302–315; (*m*) D. Tan and F. García, *Chem. Soc. Rev.*, 2019, **48**, 2274–2292; (*n*) J. Andersen and J. Mack, *Green Chem.*, 2018, **20**, 1435–1443; (*o*) C. Bolm and J. Hernández, *ChemSusChem*, 2018, **11**, 1410–1420; (*p*) D. Tan and T. Friščić, *Eur. J. Org. Chem.*, 2018, 18–33; (*q*) J. Do and T. Friščić, *ACS Cent. Sci.*, 2017, **3**, 13–19; (*r*) J. Hernández and C. Bolm, *J. Org. Chem.*, 2017, **82**, 4007–4019; (*s*) G. Wang, *Chem. Soc. Rev.*, 2013, **42**, 7668–7700; (*t*) S. James and T. Friščić, *Chem. Soc. Rev.*, 2013, **42**, 7494–7496; (*u*) K. Ralphs, C. Hardacre and S. James, *Chem. Soc. Rev.*, 2013, **42**, 7701–7718; (*v*) S. James, C. Adams, C. Bolm, D. Braga, P. Collier, T. Friščić, F. Grepioni, K. Harris, G. Hyett, W. Jones, A. Krebs, J. Mack, L. Maini, A. Orpen, I. Parkin, W. Shearouse, J. Steed and D. Waddell, *Chem. Soc. Rev.*, 2012, **41**, 413–447.

2 For selected examples of mechanochemical studies recently see: (*a*) K. Kubota, J. Jiang, Y. Kamakura, R. Hisazumi, T. Endo, D. Miura, S. Kubo, S. Maeda and H. Ito, *J. Am. Chem. Soc.*, 2024, **146**, 1062–1070; (*b*) K. Kubota, T. Endo and H. Ito, *Chem. Sci.*, 2024, **15**, 3365–3371; (*c*) F. Cuccu, F. Basoccu, C. Fattuoni and A. Porcheddu, *Green Chem.*, 2024, **26**, 1927–1934; (*d*) F. Cuccu and A. Porcheddu, *Green Chem.*, 2024, **26**, 2684–2691; (*e*) S. Pan, F. Mulks, P. Wu, K. Rissanen and C. Bolm, *Angew. Chem., Int. Ed.*, 2024, **63**, e2023167; (*f*) J. Templ and M. Schnürch, *Angew. Chem., Int. Ed.*, 2024, **63**, e2023146; (*g*) G. Shao, P. Li, Z. Yin, J. Chen, X. Xia and G. Wang, *RSC Mechanochem.*, 2024, DOI: **10.1039/D3MR00010A**; (*h*) T. Čarný, P. Kisszékelyi, M. Markovič, T. Gracza, P. Kóoš and R. Šebesta, *Org. Lett.*, 2023, **25**, 8617–8621; (*i*) T. Seo, K. Kubota and H. Ito, *J. Am. Chem. Soc.*, 2023, **145**, 6823–6837; (*j*) X. Gu, T. Wang and K. Yan, *Org. Lett.*, 2023, **25**, 7287–7292; (*k*) H. Luo, F. Liu, Y. Liu, Z. Chu and K. Yan, *J. Am. Chem. Soc.*, 2023, **145**, 15118–15127; (*l*) C. Lennox, T. Borchers, L. Gonnet, C. Barrett, S. Koenig, K. Nagapudi and T. Friščić, *Chem. Sci.*, 2023, **14**, 7475–7481; (*m*) M. Passia, M. Amer, J. Demaerel and C. Bolm, *ACS Sustainable Chem. Eng.*, 2023, **11**, 6838–6843; (*n*) C. Chen, J. Chen and C. To, *Green Chem.*, 2023, **25**, 2559–2562; (*o*) C. Patel, E. André-Joyaux, J. Leitch, X. Irujo-Labalde, F. Ibba, J. Struijs, M. Ellwanger, R. Paton, D. Browne, G. Pupo, S. Aldridge, M. Hayward and V. Gouverneur, *Science*, 2023, **381**, 302–306; (*p*) P. Bonn, J. Ke, C. Weike, J. Ward, K. Rissanen and C. Bolm, *CCS Chem.*, 2023, **5**, 1737–1744.

3 (*a*) F. Gomollón-Bel, *Chem. Int.*, 2019, **41**, 12–17; (*b*) F. Gomollón-Bel and J. García-Martínez, *Nat. Chem.*, 2022, **14**, 113–114.

4 For selected reviews discussing green metric assessment in mechanochemistry see: (*a*) N. Fantozzi, J. Volle, A. Porcheddu, D. Virieux, F. García and E. Colacino, *Chem. Soc. Rev.*, 2023, **52**, 6680–6714; (*b*) K. Ardila-Fierro and J. Hernández, *ChemSusChem*, 2021, **14**, 2145–2162.

5 For selected examples discussing green metric assessment in mechanochemistry see: (*a*) Z. Zhao, S. Ikawa, S. Mori, Y. Sumii, H. Adachi, T. Kagawa and N. Shibata, *ACS Sustainable Chem. Eng.*, 2024, **12**, 3565–3574; (*b*) V. Canale, M. Kamiński, W. Trybała, M. Abram, K. Marciniec, X. Bantreil, F. Lamaty, J. Parkitna and P. Zajdel, *ACS Sustainable Chem. Eng.*, 2023, **11**, 16156–16164; (*c*) L. Pontini, J. Leitch and D. Browne, *Green Chem.*, 2023, **25**, 4319–4325; (*d*) S. Niu, W. Yuan, X. Gong, B. Bao, Z. Wu, B. Xu, R. Zeng, Q. Yang and Q. Ouyang, *ACS Sustainable Chem. Eng.*, 2023, **11**, 17816–17825; (*e*) X. Yang, H. Wang, Y. Zhang, W. Su and J. Yu, *Green Chem.*, 2022, **24**, 4557–4565.

6 D. Hasa, G. S. Rauber, D. Voinovich and W. Jones, *Angew. Chem., Int. Ed.*, 2015, **54**, 7371–7375.

7 (*a*) G. Bowmaker, *Chem. Commun.*, 2013, **49**, 334–348; (*b*) T. Friščić, S. Childs, S. Rizvi and W. Jones, *CrystEngComm*, 2009, **11**, 418–426.

8 For selected examples discussing liquid-assisted grinding see: (*a*) J. Jia, Q. Wang, J. Li, Z. Xu, H. Li, D. Wei and B. Yuan, *ACS Sustainable Chem. Eng.*, 2024, **12**, 111–119; (*b*) M. Williams, L. Morrill and D. Browne, *Adv. Synth. Catal.*, 2023, **365**, 1477–1484; (*c*) Y. Hou, H. Wang, J. Xi, R. Jiang, L. Zhang, X. Li, F. Sun, Q. Liu, Z. Zhao and H. Liu, *Green Chem.*, 2023, **25**, 2279–2286; (*d*) T. Peňaška, V. Modrocká, K. Stankovianska, M. Mečiarová, E. Rakovský and R. Šebesta, *ChemSusChem*, 2022, **15**, e2022000; (*e*) T. Seo, N. Toyoshima, K. Kubota and H. Ito, *J. Am. Chem. Soc.*, 2021, **143**, 6165–6175.

9 (*a*) Q. Cao, J. Howard, D. Crawford, S. James and D. Browne, *Green Chem.*, 2018, **20**, 4443–4447; (*b*) J. Howard, Y. Sagatov, L. Repusseau, C. Schotten and D. Browne, *Green Chem.*, 2017, **19**, 2798–2802.

10 P. Ying, T. Ying, H. Chen, K. Xiang, W. Su, H. Xie and J. Yu, *Org. Chem. Front.*, 2024, **11**, 127–134.

11 (*a*) K. Kubota, T. Seo and H. Ito, *Faraday Discuss.*, 2023, **241**, 104–113; (*b*) L. Germann, S. Emmerling, M. Wilke, R. Dinnebier, M. Moneghini and D. Hasa, *Chem. Commun.*, 2020, **56**, 8743–8746; (*c*) D. Scaramuzza, G. Rauber, D. Voinovich and D. Hasa, *Cryst. Growth Des.*, 2018, **18**, 5245–5253; (*d*) A. Mascitti, M. Lupacchini, R. Guerra, I. Taydakov, L. Tonucci, N. d'Alessandro, F. Lamaty,

 This journal is © The Royal Society of Chemistry 2024

Published on 09 2024. Downloaded on 26-11-2025 15:26:21.

J. Martinez and E. Colacino, *Beilstein J. Org. Chem.*, 2017, **13**, 19–25.
12 V. Declerck, E. Colacino, X. Bantreil, J. Martinez and F. Lamaty, *Chem. Commun.*, 2012, **48**, 11778–11780.
13 (*a*) S. Mkrtchyan, V. Purohit, J. Zapletal, O. Shalimov and V. Iaroshenko, *ACS Sustainable Chem. Eng.*, 2024, **12**, 1–9; (*b*) U. Kanchana, E. J. Diana, T. Mathew and G. Anilkumar, *Carbohydr. Res.*, 2020, **489**, 107954; (*c*) Ö. Laçin, J. Kwiczak-Yiğitbaşı, M. Erkan, Ş. Cevher and B. Baytekin, *Polym. Degrad. Stab.*, 2019, **168**, 108945; (*d*) K. Cousin, S. Menuel, E. Monflier and F. Hapiot, *Angew. Chem., Int. Ed.*, 2017, **56**, 10564–10568; (*e*) S. Menuel, B. Léger, A. Addad, E. Monfliera and F. Hapiot, *Green Chem.*, 2016, **18**, 5500–5509.
14 (*a*) R. Heck, *Acc. Chem. Res.*, 1979, **12**, 146–151; (*b*) R. Heck, *Org. React.*, 1982, **27**, 345–390; (*c*) I. Beletskaya and A. Cheprakov, *Chem. Rev.*, 2000, **100**, 3009–3066; (*d*) M. Oestreich, *The Mizoroki–Heck Reaction*, Wiley, New York, 2009.
15 (*a*) Y. Li and G. Yin, *Acc. Chem. Res.*, 2023, **56**, 3246–3259; (*b*) T. Kochi, S. Kanno and F. Kakiuchi, *Tetrahedron Lett.*, 2019, **60**, 150938; (*c*) H. Sommer, F. Juliá-Hernández, R. Martin and I. Marek, *ACS Cent. Sci.*, 2018, **4**, 153–165; (*d*) E. Larionov, H. Li and C. Mazet, *Chem. Commun.*, 2014, **50**, 9816–9826; (*e*) A. Dounay and L. Overman, *Chem. Rev.*, 2003, **103**, 2945–2964.
16 (*a*) M. Hilton, L. Xu, P. Norrby, Y. Wu, O. Wiest and M. Sigman, *J. Org. Chem.*, 2014, **79**, 11841–11850; (*b*) J. Knowles and A. Whiting, *Org. Biomol. Chem.*, 2007, **5**, 31–44.
17 J. Delcamp, A. Brucks and M. White, *J. Am. Chem. Soc.*, 2008, **130**, 11270–11271.
18 Z. Li, Y. Zhang and Z. Liu, *Org. Lett.*, 2012, **14**, 74–77.
19 Z. Jiang, L. Zhang, C. Dong, Z. Cai, W. Tang, H. Li, L. Xu and J. Xiao, *Adv. Synth. Catal.*, 2012, **354**, 3225–3230.
20 M. Lu, X. Chen, H. Xu, H. Dai and J. Yu, *Chem. Sci.*, 2018, **9**, 1311–1316.
21 S. Maity, P. Dolui, R. Kancherla and D. Maiti, *Chem. Sci.*, 2017, **8**, 5181–5185.
22 S. Jambu, C. Shambhavi and M. Jeganmohan, *Org. Lett.*, 2021, **23**, 2964–2970.
23 E. Werner and M. Sigman, *J. Am. Chem. Soc.*, 2010, **132**, 13981–13983.
24 (*a*) V. Bhoyare, E. Carrizo, C. Chintawar, V. Gandon and N. Patil, *J. Am. Chem. Soc.*, 2023, **145**, 8810–8816; (*b*) C. K. Giri, S. Mondal and M. Baidya, *Chem. – Asian J.*, 2023, **18**, e202300243; (*c*) J. Han, X. Sun, X. Wang, Q. Wang, S. Hou, X. Song, Y. Wei, R. Wang and W. Ji, *Org. Lett.*, 2020, **22**, 1480–1484; (*d*) W. Li, C. Li, H. Xiong, Y. Liu, W. Huang, G. Ji, Z. Jiang, H. Tang, Y. Pan and Y. Ding, *Angew. Chem., Int. Ed.*, 2019, **58**, 2448–2453; (*e*) Y. Zhou, Y. Wang, L. Ning, Z. Ding, W. Wang, C. Ding, R. Li, J. Chen, X. Lu, Y. Ding and Z. Zhan, *J. Am. Chem. Soc.*, 2017, **139**, 3966–3969; (*f*) R. Li, Z. Ding, C. Li, J. Chen, Y. Zhou, X. An, Y. Ding and Z. Zhan, *Org. Lett.*, 2017, **19**, 4432–4435; (*g*) R. Sharma, R. Kumar, I. Kumar and U. Sharma, *Eur. J. Org. Chem.*, 2015, 7519–7528; (*h*) C. Hu, K. Xiang, T. Ying and J. Yu, *Adv. Synth. Catal.*, 2024, DOI: **10.1002/adsc.202400014**.
25 K. Xiang, P. Ying, T. Ying, W. Su and J. Yu, *Green Chem.*, 2023, **25**, 2853–2862.
26 Previously, there was almost no use of oxidative Heck reaction to synthesis 3 with selectivity challenge, we only found some examples of synthesizing **3h**. (*a*) Z. Zhou, Z. Hou, F. Yang and B. Yao, *Tetrahedron*, 2018, **74**, 7228–7236; (*b*) X. Mi, M. Huang, H. Guo and Y. Wu, *Tetrahedron*, 2013, **69**, 5123–5128; (*c*) P. Sun, Y. Zhu, H. Yang, H. Yan, L. Lu, X. Zhang and J. Mao, *Org. Biomol. Chem.*, 2012, **10**, 4512–4515; (*d*) Y. Jung, R. Mishra, C. Yoon and K. Jung, *Org. Lett.*, 2003, **5**, 2231–2234.
27 The NIST X-ray Photoelectron Spectroscopy Database Online: **https://srdata.nist.gov/xps/SpectralByElm/Pd**, (accessed February 2024).
28 (*a*) F. Singh and T. Wirth, *Org. Lett.*, 2011, **13**, 6504–6507; (*b*) T. Furukawa, T. Yanagi, A. Kaga, H. Saito and H. Yorimitsu, *Helv. Chim. Acta*, 2021, **104**, e202100195; (*c*) D. Meena, Deepa, M. Aalam, P. Chaudhary, G. Yadav and S. Singh, *Polyhedron*, 2022, **222**, 115931; (*d*) J. Yu, H. Shou, W. Yu, H. Chen and W. Su, *Adv. Synth. Catal.*, 2019, **361**, 5133–5139; (*e*) P. Liu, Y. Pan, K. Hu, X. Huang, Y. Liang and H. Wang, *Tetrahedron*, 2013, **69**, 7925–7930.
29 (*a*) E. Werner and M. Sigman, *J. Am. Chem. Soc.*, 2011, **133**, 9692–9695; (*b*) Y. Zou and J. Zhou, *Chem. Commun.*, 2014, **50**, 3725–3728.
30 L. Wei, J. Zhang and L. Xu, *ACS Sustainable Chem. Eng.*, 2020, **8**, 13894–13899.